Available online at www.sciencedirect.com
SCIENCE DIRECT®
Journal of Power Sources 118 (2003) 96–107
JOURNAL OF POWER SOURCES
www.elsevier.com/locate/jpowsour

A global thermo-electrochemical model for SOFC systems design and engineering

L. Petruzzi*, S. Cocchi, F. Fineschi

Dipartimento di Ingegneria Meccanica, Nucleare e della Produzione, Università di Pisa, via Diotisalvi 2, Pisa 56126, Italy

Abstract

At BMW AG in Munich high-temperature solid oxide fuel cells (SOFCs) are being developed as an auxiliary power unit (APU) for high-class car conveniences. Their design requires simulation of their thermo-electrochemical behaviour in all the conditions that may occur during operation (i.e. heat-up to about 600 °C, start-up to operating temperature, energy-delivering and cool-down). A global thermo-electrochemical model was developed for the whole system and a three-dimensional geometry code was performed using MATLAB programming language. The problems in developing SOFCs are now so many and so different that a very flexible code is necessary. Thus, the code was not only designed in order to simulate each of the operating conditions, but also to test different stack configurations, materials, etc. In every event, the code produces a time-dependent profile of temperatures, currents, electrical and thermal power density, gases concentrations for the whole system. The heat-up and start-up simulations allow: (1) to evaluate the time the cell stack needs to reach operating temperature from an initial temperature distribution, (2) to check the steepest temperature gradients occurring in the ceramic layers (which result in material stresses) and (3) to obtain important information about the pre-operating strategy. Simulation of energy-delivering gives a detailed profile of the temperatures, currents, power density, and allows to define the guidelines in system-controlling. Simulation of cooling-down gives important advises about insulation designing. The aim of this work is to build up a tool to clearly individuate the best designing criteria and operating strategy during the development and the engineering of a SOFC system.

Keywords: Solid oxide fuel cells; Three-dimensional dynamic modelling; Stack design; Global system simulations; Auxiliary power unit

1. Introduction

A fuel cell is an energy conversion device that produces electricity (and heat) directly from a gaseous fuel by electrochemical combination of the fuel with an oxidant. Bypassing the conversion in thermal and mechanical energy, the conversion efficiency is significantly higher than conventional methods of power generation's efficiency. Other important features of fuel cells are: environmental compatibility, modularity (fuel cell efficiency is relatively independent of size), siting flexibility, quiet operation, multi-fuel capability. Solid oxide fuel cells (SOFCs) are one of the most attracting kind of fuel cells. Since the electrolyte is a ceramic layer, high operating temperature (600–1000 °C) is required to achieve a good conductivity: the advantages are a high rate in reaction kinetics, fuel reforming within the cell when the fuel is a hydrocarbon, high-quality exiting heat which can be used as heat source for other applications. Besides that, high temperature imposes stringent conditions both in designing the device and in defining its operation procedure.

In addition to high-profile SOFC applications such as automotive propulsion and distributed power generation, the use of SOFC such as auxiliary power units (APUs) for vehicles has received considerable attention. Till date, a car's conveniences are directly supplied by the engine power. Some issues are joined with this approach: the engine does not work at the designed operating conditions; fuel consumption and pollutants emission increase. An APU system would allow the avoidance of performance and efficiency losses of the engine. Moreover, engine performance improvement is expected by recycling anode exhaust to the engine itself. APU applications may also be an attractive market opportunity because it offers a true mass-market opportunity that does not require the challenging performance and low cost required for propulsion system for vehicles. The design of a SOFC stack is deeply governed by the restrictions imposed by the properties of the cell materials. All the components must also maintain adequate physical, chemical, electrical and electrochemical features at every operating conditions. A SOFC stack must

* Corresponding author. Tel.: +39-3474121927; fax: +39-050836665.
E-mail address: luca_petruzzi@libero.it (L. Petruzzi).

0378-7753/03/$ – see front matter
doi:10.1016/S0378-7753(03)00067-3

Nomenclature

A	surface area (m^2)
C_p	heat capacity (J/(kg K))
D	equivalent channel diameter (m)
E	cell voltage (V)
E_r	reversible voltage (V)
F	Faraday's constant (J/(mol K))
h	heat-transfer coefficient (W/(m^2 K))
ΔH	reaction enthalpy (J/kg)
I	current (A)
k	thermal conductivity (W/(m K))
K	pre-exponential factor (A/m^2)
$\dot{m}$	specific mass flow (kg/(s m^2))
n	electrons exchanged
p	partial pressure (MPa)
P	power (W)
R	resistance (Ω)
s	thickness (m)
T	local temperature (K)
$\bar{T}$	average temperature (K)
U	activation energy (J/mol)
U_f	fuel utilisation

Greek symbols

ε	efficiency
ρ	mass density (kg/m^3)
σ	electric conductivity (Ω^{-1} m^{-1})

Subscripts

A	anode
c	conduction
C	cathode
conv	convection
el	electric
env	environment
f	fuel
i	stack actual layer
ijk	actual segmentation volume
in	inner insulation surface gas inlet
ins	insulation layer
lat	outer lateral stack surface
n	normal to the insulation surface
out	outer insulation surface gas outlet
ox	oxidant
r	radiation
st	stack
Sh	shifting reaction
th	thermal
vf	fuel feeding vane
w	channel wall
Ω	ohmic

be designed to achieve desired performances, mechanical integrity, manifolding and sealing requirements. Moreover, the fabrication and assembly procedures must guarantee both the required features and the possibility of the valuation that such features are being achieved. In order to obtain an efficient reliable and safe system, the thermal, mechanical, and electrochemical behaviour must be known for all the components in all the involved operating and manufacturing conditions. SOFC systems will need experimentation to reach technological maturity. Mathematical and numerical modelling permit the prediction of the cell, stack and system behaviour under several conditions, investigating the relative weight of the operating and manufacturing parameters. Thus, the research and development efforts can be conveniently directed.

This work, which was carried out in Munich (Germany) at BMW AG, is concerned about the design of a SOFC stack to be used as APU system. A simulating code is developed in order to investigate the system's thermo-electrochemical behaviour under several operating conditions. The aim of this work is to build up a tool to clearly individualise the best system designing criteria and operating strategy.

2. General features of the APU

The SOFC stack requires of external devices to operate (Figs. 1–3). Since the whole system has to be mounted on a car, important requirements are: low system complexity, low weight and size, high reliability, fast start-up time, safe operating, low cost compared with the vehicle one. Using the same fuel for the thermal engine as for the stack, i.e. usual petrol, eliminating the presence of a second fuel tank. Petrol must be processed in a proper fuel processor before being fed into the stack. In the simplified layout of the system the fuel processor is assumed to be utilised not only to provide fuel during energy-delivering conditions, but also as a petrol-burner producing the hot exhaust gases which carry out the heating-up procedure. Besides that, a heat exchanger is necessary in order to have an additional control tool for heating-up procedures: especially at the first heat-up, the very large temperature difference between the hot gases and the stack may induce in the cells such steep temperature gradients as to damage them. A failure in the cells makes the

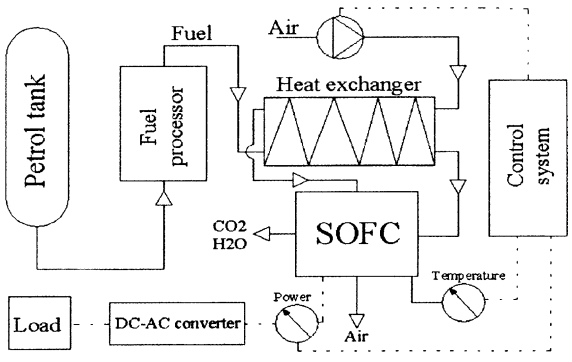

Fig. 1. APU schematic layout.

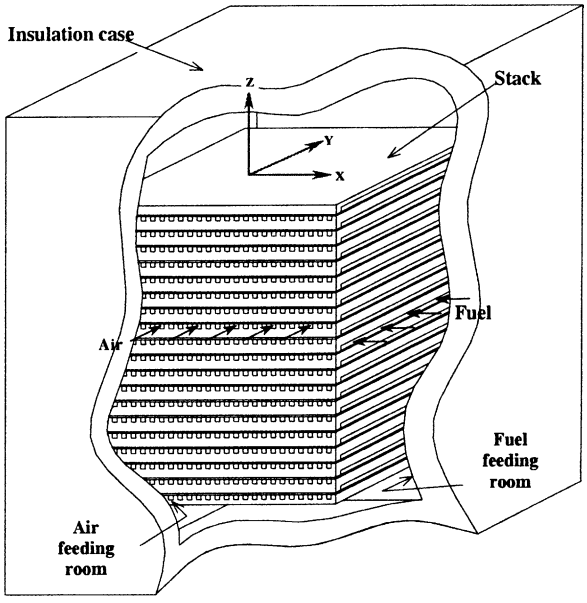

Fig. 2. SOFC schematic configuration.

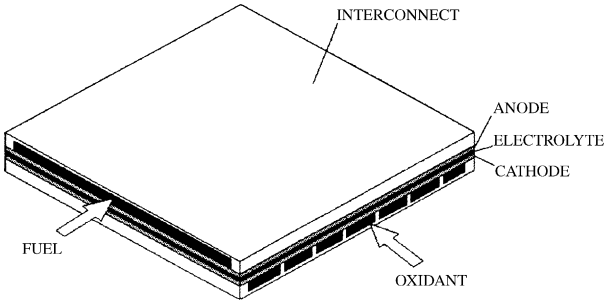

Fig. 3. Single cell.

fuel and oxidant come into contact, at a temperature which can promote a disruptive explosion.

2.1. Management system

A rapid feedback control system checks the main parameters for the system operating (i.e. the stack average temperature, the power delivered, the fuel and oxidant flows) and manages them in order to follow the external load, maintaining the stack temperature as close as possible to the planned value. The main controlling tool is the oxidant mass flow, since it may also act as a coolant.

2.2. Fuel processor

Current thinking is that reformers for SOFC–APUs will be of the exothermic type (i.e. partial oxidation or autothermal reforming). Even if a steam reformer could improve the efficiency of the fuel processing procedure, the thermal management of the system would be deeply complicated (the steam reforming reactions are strongly endothermic). The reference composition of the reformate is computed assuming the use of a POX system [1].

2.3. SOFC system

The system, being at its first steps of designing, has only been configured at a low detail level. Fixed features are the flat-plate design, the cross-flow configuration, and the cell materials. A single cell is assumed to be 0.15 m × 0.15 m. The reference fuel mixture consists of 24% CO, 26% H_2, 46% N_2, 1.5% H_2O, 2.5% CO_2 volume. Nominal operating conditions are the following: 3.5 kW electric power, 80–85% fuel utilisation, 35% system efficiency, 800 °C average stack temperature.

According to Fig. 4, a first measuring of the stack can be done. For instance, at 800 °C and 0.8 V, the single cell electrical power would be about 72 W (320 mW/cm^2). Assuming that car convenience systems require about 3.5 kW, the stack must be made of 50 cells. Such a stack results in a good compromise between increasing voltage (i.e. reducing polarisation losses, thus increasing efficiency) and keeping the stack surface-to-volume ratio to a low value (facilitating the stack thermal insulation).

The single cell (see Fig. 3) is constituted by a membrane electrolyte assembly (MEA), consisting of a ceramic electrolyte sandwiched between an anode and a cathode, a fuel channel directly faced to the anode, a set of oxidant channels directly faced to the cathode, and an interconnect that connects the cathode of the cell to the anode of the next cell in electrical series, in order to build up voltage. The interconnect consists of three elements: a thin porous nickel layer covers the anode; a second thicker nickel layer of high porosity acts as connecting element through the fuel channel; a metal layer directly connects the nickel layer to the cathode.

The resultant stack of cells has to be insulated by means of an external ceramic case (see Fig. 2). Insulation case is a critical SOFC component, whose characteristics affect both the cooling own time (time necessary before the stack average temperature falls below a fixed value starting from

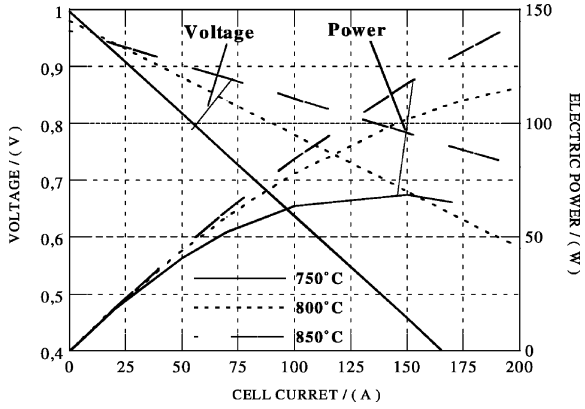

Fig. 4. Calculated characteristic curve of a single cell ($p_{CO} = 0.24$; $p_{H_2} = 0.26$; $p_{H_2O} = 0.015$; $p_{CO_2} = 0.025$; $p_{N_2} = 0.46$).

Table 1
Physical and geometrical parameters of the elements constituting the stack

	Theoretical density (kg/m^2)	Specific heat (J/(kg K))	Thermal conductivity (W/(m K))	Material	Porosity (%)	Thermal expansion coefficient (10^{-6} K^{-1})	Melting temperature (°C)	Layer thickness (mm)
Cathode	6570	573	4	$La_{1-x}Sr_xMnO_3$	20	11.2	1880	0.04
Electrolyte	5900	606	2	YSZ	<1	10.8	2680	0.07
Anode	6870	595	2	Ni-YsZ	20	12.4	1453	0.04
Ni cover-layer	8900	518	71.8	Ni	20	13.3	1455	0.2
Thicker Ni layer	8900	518	71.8	Ni	80	13.3	1455	1.15
Insulation	480	1047	0.059	Al_2O_3 85%, SiO_2 15%	93	5	1870	50

operating temperature) and the maximum temperature on the external case surface (which must be kept below 100 °C, according to the safety standards established by the manufacturing company). At present, the most reasonable choice as insulating material seems to be the ceramic in Table 1; however, an indication whether such a solution is adequate or not is expected to come from system's thermal simulation.

The most important physical properties of the SOFC component materials are listed in Table 1.

3. Simulation model

A strict model of the SOFC stack requires the description of complex physical and electrochemical phenomena. Most of such phenomena are joined together and some simplifications must be done to obtain the equations and the boundary conditions describing them. It is no easy to perform a global model and to implement it in an unique code. The developed model allows to evaluate, with different levels of detail, the time- and space-dependent profile of the thermodynamic and electrochemical quantities (temperature, molar fraction, thermal power density, polarisation, current density, electrical power density). Also, the heat exchanger and the fuel processor have been simply modelled. In this manner, the model permits not only design and optimisation, but also off-design, safety and reliability analysis (Fig. 5).

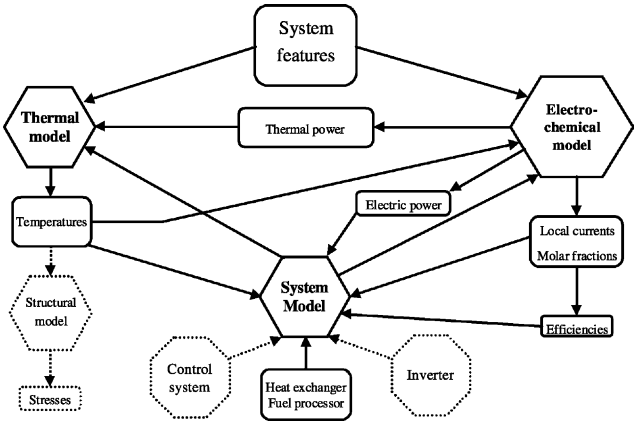

Fig. 5. Simulation model (the dashed lines indicate what is not included the developed model).

Some preliminary simplifications must be done on the geometry of the SOFC. In the considered configuration (Fig. 2) some details are neglected. Anyway, the system configuration is known just at a low level of detail, thus, it would be useless to consider a more refined representation.

3.1. Electrochemical model

The stack is assumed to be fed by partial oxidised petrol, which means that the following species are considered: carbon dioxide (CO_2), carbon monoxide (CO), water (H_2O), hydrogen (H_2) and nitrogen (N_2).

The following chemical reactions are assumed to be relevant:

$$H_2 + \tfrac{1}{2}O_2 \rightarrow H_2O \quad (1)$$

$$CO + \tfrac{1}{2}O_2 \rightarrow CO_2 \quad (2)$$

$$CO + H_2O \rightarrow CO_2 + H_2 \quad (3)$$

Methane (CH_4) can also be included in the inlet gas composition and the steam reforming reaction inside the stack can be considered. This allows easy application of the model and the implemented code to natural gas fuelled SOFC systems.

3.1.1. Electrochemical oxidation of CO

Compared to the hydrogen reaction, the oxidation of CO at SOFC operating temperatures is accompanied by higher overpotentials [2]. The presence of CO_2 lowers such overpotentials; the role of CO_2 in the CO oxidation is similar to that of H_2O in the H_2 oxidation. However, in the presence of H_2O, the favourable path for the oxidation of CO is generating hydrogen by the water shift reaction. Thus, for gas mixture that contains H_2, H_2O and CO, the anode is expected to have overpotential comparable to that for H_2/H_2O mixtures [3]. Many parameters influence this issue and experimental tests should be done to perform a strict model. Two different approaches have been developed: the first one considers only the water shift reaction of CO, while the second one consider both the electrochemical oxidation of CO and the water shift reaction. Results from these two extreme approaches are compared. However, such phenomena should be deeply investigated both carrying

Table 2
Steady-state operating conditions according to the first and the second approach (see Section 3.1.1)

	H_2 and CO reactions		H_2 reactions only	
Cell voltage (V)	0.8	0.75	0.8	0.75
Average stack temperature (°C)	800	800	800	800
Fuel utilisation (%)	0.8	0.93	0.7	0.8
Thermodynamic efficiency (%)	69.29	69.12	75.83	75.83
Electric power (W)	72.2	80.9	62.9	70
Cell efficiency (%)	45	50.6	43.3	48.12

out experimentation and performing semi-empirical models. In fact, the amount of electrochemical reacting CO influences the overall performances of the system (see Table 2).

3.1.2. Assumptions

- All the polarisations are considered to be linear with current density.
- Operating voltage is assumed to be uniform over the whole surface of the cell.
- All the cells are assumed to work at the same operating voltage (actually the voltage distribution is connected to temperature distribution; such an effect can be evaluated separately).
- Concentration and diffusion polarisation due to mass transport effect is neglected; such polarisation becomes important at low concentration of the reactant gases and high value of current density. This system is not expected to operate in such conditions (actually such phenomena should be taken into account if the CO electrochemical reaction is considered).
- No contact resistance between individual cell components is taken into account.
- All the thermal power is assumed to be delivered into the MEA.

3.1.3. Polarisations

When the fuel cell delivers electrical energy to an external circuit, the voltage no longer corresponds to the reversible one, but drops down because of the occurrence of irreversibility in conversion from chemical into electrical energy. The voltage drop with increasing current density is due to the sum of several phenomena [1,2,5]. *Activation polarisation* represents the extrapotential necessary to reduce the energy barrier of the rate-determining step of the reaction to a value such that the electrode reaction proceeds at a desired rate. Such polarisation is related to current density, i, by the Tafel equation. A linear approach is applicable if the equilibrium potential change is small. Anodic and cathodic equivalent resistances are calculated for every segmented volume [4]:

$$R_{\mathrm{C}} = \left[\frac{4F}{RT}k_{\mathrm{C}}\left(\frac{p_{\mathrm{O_2}}}{p}\right)^{0.25}\exp\left(-\frac{U_{\mathrm{C}}}{RT}\right)\right]^{-1} \tag{4}$$

$$R_{\mathrm{AH_2}} = \left[\frac{4F}{RT}k_{\mathrm{AH_2}}\left(\frac{p_{\mathrm{H_2}}}{p}\right)^{0.25}\exp\left(-\frac{U_{\mathrm{A}}}{RT}\right)\right]^{-1} \tag{5}$$

$$R_{\mathrm{ACO}} = \left[\frac{4F}{RT}k_{\mathrm{ACO}}\left(\frac{p_{\mathrm{CO}}}{p}\right)^{0.25}\exp\left(-\frac{U_{\mathrm{A}}}{RT}\right)\right]^{-1} \tag{6}$$

A test session should be performed on a MEA layer over a large range of operating temperatures and gas compositions in order to provide the pre-exponential factors and the activation energies for the Eqs. (4)–(6). The stack, not already being available, such figures are calculated assuming certain MEA performances at nominal operating conditions (Fig. 4). *Ohmic polarisation* is caused by resistance to the conduction of ions (through the electrolyte) and electrons (through the electrodes and the interconnects), and by the contact resistance between the cell components. The ohmic resistance is calculated from the conductivity (values from [6]) of individual layers and is given by:

$$R_{ijk} = \frac{s_{ijk}}{\sigma_{ijk}A_{ijk}} \tag{7}$$

3.1.4. Currents

Current distribution is the main unknown of the electrochemical model. Once such a quantity is known, the other quantities (gases composition, efficiencies, fuel utilisation, thermal power density, electric power density) can be calculated.

According to the first approach (see Section 3.1.1), a single cell can be schematised with the equivalent circuit shown in Fig. 6. The following equation can be write for every segmented volume:

$$I_{ijk} = \frac{E_{\mathrm{rH_2}} - E}{R_{\mathrm{C}} + R_{\mathrm{AH_2}} + R_{\Omega}} \tag{8}$$

According to the second approach (see Fig. 6), current from the electrochemical reaction of CO, I_{CO}, has to be considered. The three unknowns I, $I_{\mathrm{H_2}}$, I_{CO}, can be calculated from the following equations:

$$\begin{aligned} E &= E_{\mathrm{rH_2}} - (R_{\Omega}I + R_{\mathrm{AH_2}}I_{\mathrm{H_2}} + R_{\mathrm{C}}I) \\ E &= E_{\mathrm{rCO}} - (R_{\Omega}I + R_{\mathrm{ACO}}I_{\mathrm{CO}} + R_{\mathrm{C}}I) \\ I &= I_{\mathrm{H_2}} + I_{\mathrm{CO}} \end{aligned} \tag{9}$$

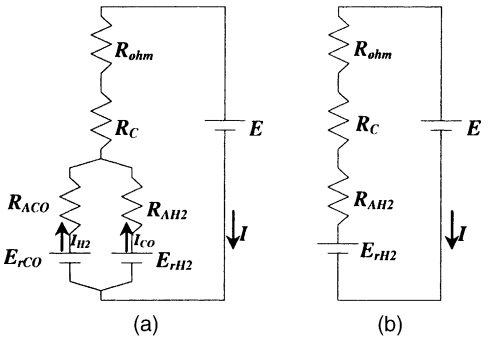

Fig. 6. Equivalent circuit for the second (a) and the first (b) approach.

3.1.5. Molar fractions

Mass balances are formulated for each species linking the local current, I_{ijk} with the change in concentration of the reacting species. Five balance equations can be written according to Eqs. (1)–(3):

$$\begin{aligned} N_{\mathrm{CO},(i+1)jk} &= N_{\mathrm{CO},ijk} - x - z \\ N_{\mathrm{CO_2},(i+1)jk} &= N_{\mathrm{CO_2},ijk} + x + z \\ N_{\mathrm{H_2},(i+1)jk} &= N_{\mathrm{H_2},ijk} + x - y \\ N_{\mathrm{H_2O},(i+1)jk} &= N_{\mathrm{H_2O},ijk} - x + y \\ N_{\mathrm{O_2},(i+1)jk} &= N_{\mathrm{O_2},ijk} - \tfrac{1}{2}y - \tfrac{1}{2}z \end{aligned} \tag{10}$$

where x, y and z are the rates of the shift reaction, the H_2 electrochemical reaction and the CO electrochemical reaction. The shift reaction is always assumed to be at equilibrium. Thus, the following equation can be written:

$$K_{\mathrm{eq,CO}} = \frac{N_{\mathrm{H_2},ijk} N_{\mathrm{CO_2},ijk}}{N_{\mathrm{CO},ijk} N_{\mathrm{H_2O},ijk}} \tag{11}$$

The equilibrium constant can be described as a function of temperature according to [7]. The remaining two equations relate local currents to y and z:

$$y = \frac{I_{\mathrm{H_2},ijk}}{nF}, \qquad z = \frac{I_{\mathrm{CO},ijk}}{nF} \tag{12}$$

Whether the electrochemical reaction of CO is not considered, z has to be kept equal to zero.

3.1.6. Electric power and efficiencies

The electric power produced by a cell is simply the sum of local currents, multiplied by the cell voltage:

$$P_{\mathrm{el}} = \sum_{ijk} I_{ijk} E \tag{13}$$

cell efficiency is given by

$$\varepsilon = \frac{P_{\mathrm{el}}}{N_{\mathrm{f,in}} \mathrm{LHV_f}} \tag{14}$$

fuel utilisation is defined by the following equation:

$$U_{\mathrm{f}} = \frac{N_{\mathrm{H_2,in}} + N_{\mathrm{CO,in}} - N_{\mathrm{H_2,out}} - N_{\mathrm{CO,out}}}{N_{\mathrm{H_2,in}} + N_{\mathrm{CO,in}}} \tag{15}$$

3.1.7. Thermal power density

The heat generation into the stack is due to the chemical reactions, the water shift reaction and the ohmic resistance. Not all the reaction enthalpy is converted into electric energy: one part is absorbed by the reaction products, as entropy productions and another part is dissipated into the cell components, as a result of polarisation phenomena. The first of such a heat is linked to the so called thermodynamic efficiency and is delivered into the reaction zone. It is reasonable to suppose the such heat is directly generated into the electrode. The heat-transfer coefficient between fuel and electrode is high enough to consider all the heat left to the gasses is deposited into the same element volume in which it is generated. Under the further hypothesis that the heat generated into interconnect layers is low, heat generation is present only in the MEA layers:

$$\begin{aligned} P_{\mathrm{th}} = {} & x\,\Delta H_{\mathrm{sh}} + I^2(R_\Omega + R_{\mathrm{C}}) + I_{\mathrm{H_2}}^2 R_{\mathrm{AH_2}} + I_{\mathrm{CO}}^2 R_{\mathrm{ACO}} \\ & + T(y\,\Delta H_{\mathrm{H_2}} + z\,\Delta H_{\mathrm{CO}}) \end{aligned} \tag{16}$$

3.2. Thermal model

3.2.1. Balance equations

Relating to an O(xyz) frame of reference in which fuel and oxidant channel axes individuate respectively x- and y-axes (Fig. 2), conservation equations may be expressed in a differential form by means of partial derivative equations (PDEs), one for each stack component.

3.2.1.1. Stack solid layers. Stack solid layers are described only by means of the energy-balance equation:

$$\rho_i C_{p,i} \frac{\partial T_i(x,y,z,t)}{\partial t} = \vec{\nabla} k_i(T_i)\, \vec{\nabla} T_i(x,y,z,t) + \frac{P_{\mathrm{th}}(x,y,z,t)}{s_i A_i} \tag{17}$$

3.2.1.2. Insulation case elements. Insulation case consists of six thick layers arranged in a closed box surrounding the stack and the gas feeding vanes. At present, the insulation case is supposed to be a solid material, thus its thermal behaviour can be described by the energy-balance equation for solid bodies (Eq. (17)).

3.2.1.3. Fuel channels. The gas mixture flow could be described by means of the equations of the classical gas-dynamics theory. Nevertheless, in such an approach not only the temperature profile but also the pressure one is unknown, doubling the effort necessary to obtain a solution. Thus, it is opportune to describe the fuel flow under the following simplifying hypotheses:

- Pressure is at a constant value along the whole channel. Pressure drops are neglected, even if they are expected to be quite large, because of the nickel layer through which the gas has to flow.

- Time-constants for gas flow are expected to be much smaller than ones for stack solid components. Thus, at any time the gas flow is supposed to be in steady-state conditions.
- In order to reduce the spatial dependence of the model, gas temperature is averaged on the section perpendicular to the flow direction: thus, spatial temperature profile varies only along the channel axis.
- At any abscissa x and for each surface limiting the channel, also wall temperature is averaged along the direction perpendicular to the channel axis.
- Heat-transfer is supposed to occur only by convection. Nevertheless, the presence of the nickel layer gives place to a parallel heat-transfer mechanism, which in turn may considers the series of heat-transfer from gas flow to nickel layer by convection and from nickel layer to the surrounding components by conduction. Moreover, especially during heat-up, radiation gives an important contribution to heat-transfer, which cannot be neglected. All these factors are taken into account using a global heat-transfer coefficient, strongly dependent on temperature and channel geometry besides nickel layer porosity, which has to be mapped with an appropriate test session. At present, only a first-guess value can be utilised as global heat-transfer coefficient, without any experimental data allowing a comparison: this actually constitutes one of the main weaknesses in the simulation code.

In the frame of the previous hypotheses, energy-balance for fuel channel may be written in the following form:

$$\dot{m}_{\mathrm{f}}(x,t)C_{p,\mathrm{f}}\frac{\partial \bar{T}_{\mathrm{f}}(x,t)}{\partial x} = -\sum_i \frac{h_{\mathrm{f}}(\bar{T}_{\mathrm{f}})}{D}(\bar{T}_{\mathrm{f}}(x,t) - \bar{T}_{\mathrm{w},i}(x,t)) \tag{18}$$

As initial condition, the average temperature in the fuel feeding vane is assigned.

3.2.1.4. Oxidant channel. All the hypotheses expressed for the fuel channel can be replicated for the oxidant channel. Thus, energy-balance equation is analogous. As initial condition, the average temperature in the oxidant feeding vane is assigned. For oxidant channels, the simplifying hypotheses are less drastic than for fuel channels. The nickel layer is not present, so a lower gas pressure drop along the channels is expected, giving a better match with the constant pressure hypothesis. The first-guess value of the global heat-transfer coefficient is assumed different from the fuel channel one, because of the different channel geometry and the absence of the nickel layer.

3.2.2. Boundary conditions

In writing boundary conditions, a further simplifying hypothesis can be made in order to avoid the complex computation of the temperatures profiles in the air and fuel feeding rooms. Heat-transfer by convection is assumed to be negligible through all the surfaces limiting such rooms. This appears to be reasonable considering that the gases inside the vanes are practically at rest.

3.2.2.1. Insulation case. In order to describe heat-transfer from the stack to the insulation case, a simplification can be made considering an average temperature for both the whole outer stack surface and the whole inner insulation surface. Two different kinds of average are required, since the different mechanisms of heat-transfer impose to conserve the two heat-fluxes separately. Thus, for the generic inner surface of the insulation case, the boundary condition is expressed in the following form:

$$\pm k_{\mathrm{ins}}\left.\frac{\partial T_{\mathrm{ins}}}{\partial n}\right|_{\mathrm{in}} = h_{\mathrm{r}}(\bar{T}^4_{\mathrm{r,st}}|_{\mathrm{lat}} - \bar{T}^4_{\mathrm{r,ins}}|_{\mathrm{in}}) + \frac{k_{\mathrm{f}}}{s_{\mathrm{vf}}}(\bar{T}_{\mathrm{c,st}}|_{\mathrm{lat}} - \bar{T}_{\mathrm{c,ins}}|_{\mathrm{in}}) \tag{19}$$

At the outer surface, the temperature must be kept below the standard value of 100 °C, thus it is reasonable to assume that heat-transfer occurs mainly by convection. The general form of the boundary condition is:

$$\pm k_{\mathrm{ins}}\left.\frac{\partial T_{\mathrm{ins}}(x,y,z,t)}{\partial n}\right|_{\mathrm{out}} = h_{\mathrm{conv}}(T_{\mathrm{ins}}(x,y,z,t)|_{\mathrm{out}} - T_{\mathrm{env}}) \tag{20}$$

3.2.2.2. Stack solid layers. Since all stack solid layers exchange heat with the fuel layer, the oxidant layer and the inner lateral insulation surface, three different types of boundary equations can be written, valid for any stack solid layer. The one describing heat-transfer with fuel channel layers is:

$$\pm k_i\frac{\partial T_i(x,y,z_{\mathrm{w},j},t)}{\partial z} = h_{\mathrm{f}}(\bar{T}_{\mathrm{f}})(\bar{T}_{\mathrm{f}}(x,t) - \bar{T}_{\mathrm{w},i}(x,t)) \tag{21}$$

Since the oxidant channel layer can be represented as an interconnect layer in which a number of rectilinear stripes have been cut to retrieve the set of oxidant channels, heat-transfer results in the combination of heat-conduction with the solid parts and heat-convection with the oxidant flow. The following simplified model is valid when the global channel volume is half the layer volume:

$$\pm k_i\frac{\partial T_i(x,y,z_{\mathrm{w},j},t)}{\partial z} = \frac{h_{\mathrm{ox}}(\bar{T}_{\mathrm{ox}})}{2}(\bar{T}_{\mathrm{ox}}(y,t) - \bar{T}_{\mathrm{w},i}(x,y,z_{\mathrm{w},j},t)) \pm \frac{k_j}{2}\frac{\partial T_j(x,y,z_{\mathrm{w},i},t)}{\partial z} \tag{22}$$

Heat-transfer within the inner lateral insulation layer can be described by means of the average temperatures discussed previously (Eq. (19)).

4. The SOFC code

In order to perform simulation of all the operating conditions, an adequate code, named SOFC, has been developed

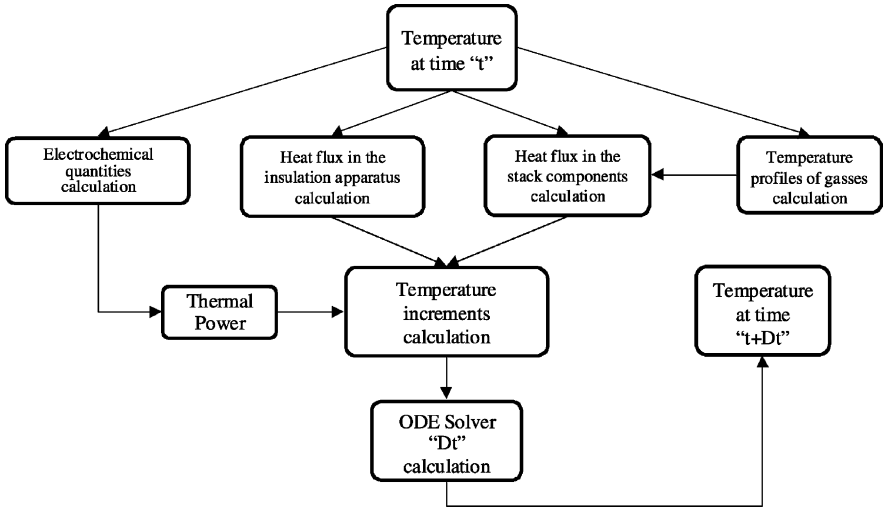

Fig. 7. Iteration procedure's schematic diagram.

using MATLAB programming language. The SOFC code is structured with functions; each of them computes specific unknown quantities (see Fig. 7). This approach easily permits improvement. Since the most important goal is to achieve a reasonably detailed map of calculated temperature representing the actual time-dependent profile (not only in the stack, but also in the insulation case), a refined three-dimensional spatial fragmentation of the whole device is necessary. MATLAB programming language has been chosen because it provides a large set of ordinary differential equation (ODE) solvers, applicable also to stiff problems as the present one, allowing the focus of all the programming efforts on the physical modelling and on the development of a good spatial fragmentation.

5. Results and discussion

All four operating conditions have been simulated and have been grouped in the following ones:

1. *Heat-up*: it consists of an energy absorption which leads the stack to the energy-delivering temperature (600 °C), starting from an initial temperature distribution which may be either room temperature or a higher one resulting after a cool-down period.
2. *Start-up*: it is the energy-delivering process occurring immediately after the onset of the electrochemical reactions (about 600 °C) and leading to steady-state operating temperature (above 800 °C).
3. *Steady-state operating*: it is the energy-delivering at constant average stack temperature, during which electrical power has to be produced following the external load.
4. *Cool-down*: it is the not-operating condition after an operating one, during which no electrical power is produced and temperature falls toward the room value.

The code permits to run simulations considering a selected number of single cells. Few cells seem to be enough to obtain good results, since the border effect influences only the upper and lower stack layers (see Fig. 8). Simulations have been carried out on simplified stacks. Even if the obtained temperature profiles are substantially correct, it is important to underline that to consider a reduced number of cells means to study a system ''less insulated'' than in the real case (Section 5.4).

5.1. Heat-up simulation

The heat-up procedure is governed by means of the following parameters: thermal power delivered by the burner, exhaust gas flow, oxidant flow, inlet temperatures, heat-transfer coefficients in the channels.

During the heat-up the fuel processor burns petrol in an air-lean atmosphere, to prevent high exhaust gas temperatures. The stack is fed by inert gasses, thus there is no thermal power generation inside the cells. When the average stack temperature reaches a certain value it becomes convenient to begin the start-up phase (feeding the fuel channel with fuel instead of exhaust gasses).

The heat-up is characterised by *heat-up time* and the *temperature gradients* in the stacks. A first simulation has been performed to reproduce heat-up by feeding the hot gases directly to the fuel channels. Results from simulation demonstrate that this heating strategy is inadequate, because it gives place to large temperature gradients that occur at the inlet of the fuel channels, especially during the first instants of heat-up. The reason for this lies in the temperature of the exhaust gases which is too high, in the low mass flow (about 6.2×10^{-5} kg/s per channel) and in the quite high values of heat-transfer coefficients, which cause a heat supplying confined into few millimetres from the channel inlet. Increasing the mass flow and reducing the inlet temperature can individualise a better heating-up strategy. This can be

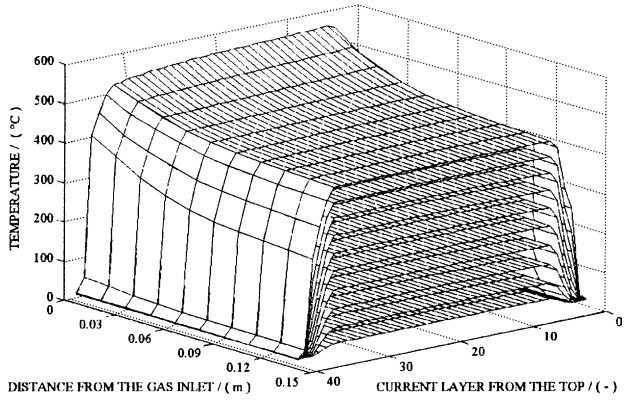

Fig. 8. Temperature profiles, during a 900 s heat-up from 25 °C, in a vertical plane parallel to the fuel channel.

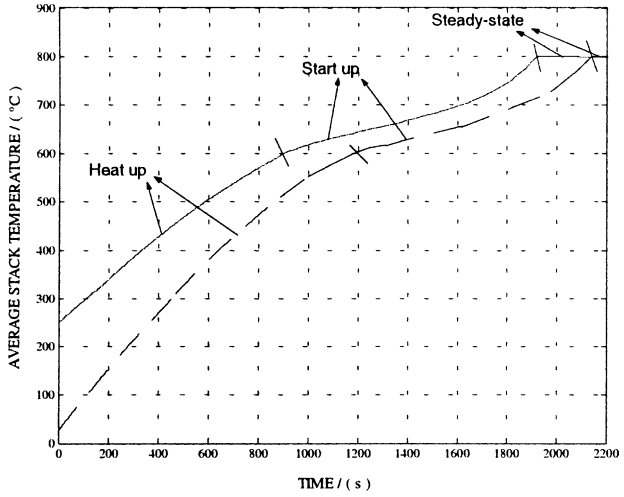

Fig. 10. Average stack temperature for all the operating conditions (continuos line, initial temperature 250 °C) and for the only heat-up (dashed line) from 25 °C.

achieved by means of exhaust gas conditioning in a heat exchanger: air, which acts as secondary fluid, can be delivered to the oxidant channels. A further advantage of this strategy is a more volume-distributed heating-up. Nevertheless, temperature gradients still occur near the inlet of the channels, even if their amplitude results to be lower. Maintaining these gradients below a reasonable value imposes a more complex heat-up procedure. The air flow in the heat exchanger must be regulated in order to achieve an inlet temperature for both the gases not too different from the stack average temperature: decreasing air mass flow to an opportune value as the average temperature increases, allows to manage the heat-up avoiding steep temperature gradients and keeping the time necessary to carry out the whole procedure within reasonable limit. The disadvantage related to this strategy is the heat exchanger, which risks to heavily complicate the whole management system. The temperature profiles achieved using the second strategy are reported in Figs. 8 and 9.

Using a burner power of about 5 kW, the heat-up time is 15 min starting from average stack temperature of 250 °C and 20 min starting from 25 °C (see Fig. 10). These values are surely too high for an automotive application (Section 5.2).

The burner power must be incremented fill the heat-up time reaches the desired value.

The SOFC code allows to optimise the parameters governing the heat-up phase, once maximum temperature gradients and heat-up time are fixed. Fig. 11 shows the temperature profiles for different burner powers. It is important to underline that temperature gradients do not increase much increasing the burner power and keeping constant the inlet gas temperatures (thus increasing the mass flow). In fact, the heat is delivered more gradually along the channels.

The value of the heat-transfer coefficient, h_f cannot be computed analytically, because of the nickel layer. Its value has a large influence on the temperature gradients. Experimentation would be necessary in order to perform an empirical relation between h_f and the parameters characterising the fuel channel (fuel flow, channel dimensions, nickel layer porosity). Such parameters could be included in the heat-up procedure optimisation.

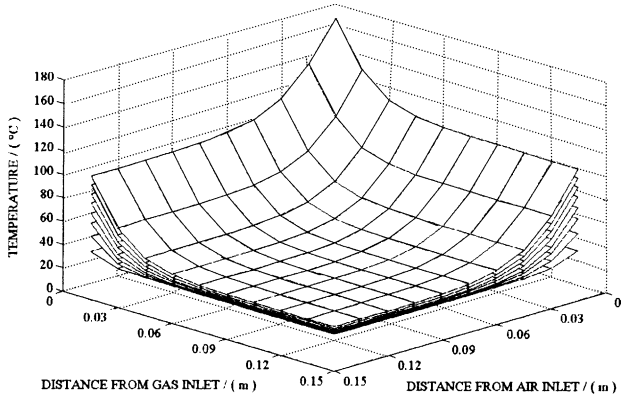

Fig. 9. Temperature behaviour in the MEA layer during the first 50 s of the heating-up from 25 °C.

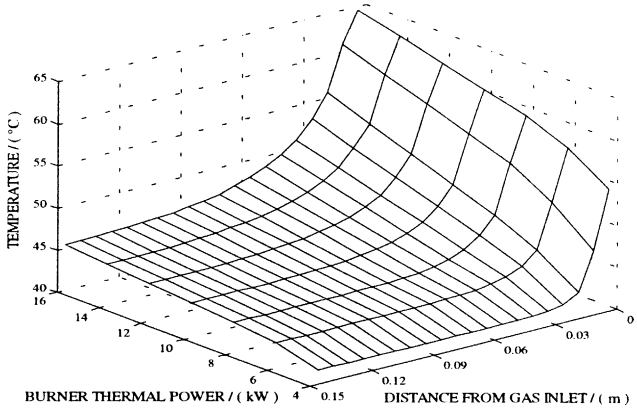

Fig. 11. Temperature profile in the MEA layer during heat-up as a function of burner thermal power.

A mechanical simulation of the heat-up would achieve to evaluate the thermal stresses and thus to fix a threshold for the temperature gradients on the base of a certain breaking criteria. However, such a model can be developed separately.

5.2. Start-up simulation

The APU system has to be managed in order to reach the steady-state operating temperature as soon as possible. Thus, when the stack temperature values are such as the heat deposited by the hot gasses is less than the heat achievable by the electrochemical reactions at such temperatures, it is convenient to switch the exhaust gas to the fuel. During start-up it is opportune to operate at the maximum thermal power. The control system must impose a low cell voltage (i.e. low electric efficiency and high thermal power). Cell voltage and fuel mass flow can be managed, during start-up in order to obtain the fastest procedure. Thus, start-up simulation can also be a good tool for the control system designing and optimisation [8]. For instance, once the fuel utilisation is fixed, the inlet fuel mass flow versus time profile during the whole phase can be individualise.

Fig. 10 shows the average stack temperature behaviour during the start-up procedure. The most convenient average temperature value to start the start-up procedure is about 600 °C.

The overall time to reach steady-state is too high for an APU system. It could be necessary to provide the system with the possibility to deliver a certain amount of electric power directly from the engine before APU reaches the steady-state.

5.3. Steady-state operating simulation

A steady-state condition can be fixed by means of the following parameters: *cell voltage*, *fuel mass flow*, *average stack temperature*. The code permits computation of the air mass flow value to obtain steady-state (i.e. the heat generated is equal to the heat removed by the gas flows). There are two possibilities to perform the steady-state simulation. Time-dependent simulations can be performed starting from the temperature pattern achieved at the end of the start-up procedure, i.e. for an average stack temperature of 800 °C. A temperature profile rearrangement occurs that tends to match an equilibrium profile imposed by fuel and oxidant gas flows (both the inlet temperatures are 700 °C). This approach makes sense only to perform simulation of transients. A simpler procedure can be developed to directly compute the steady condition (i.e. efficiencies, electric power, temperature profiles). A normal convergence iteration on the temperatures can be performed. Simulations have been carried out for both the two approaches introduced in Section 3.1.1. Table 2 shows results of steady-state simulations performed at different cell voltage. It is assumed that the external load imposes the voltage value (see Section 3.1.2) in order to simplify the electrochemical computation procedure. If CO electrochemical reactions occur the fuel utilisation increases, On the other hand, the performances of the stack declines. In effect, the thermodynamic efficiency involved in the CO reaction is lower than the H_2 one [2].

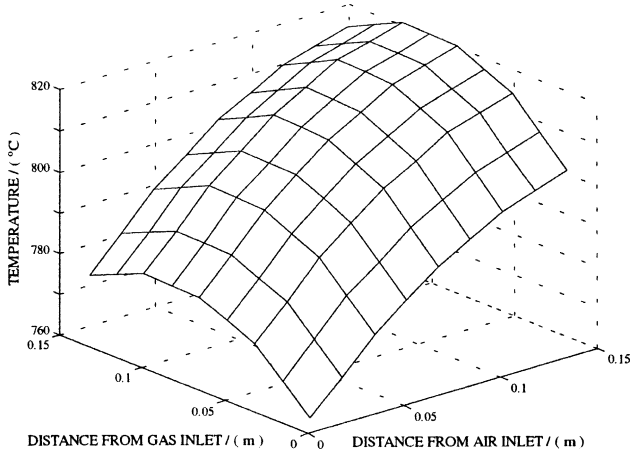

Fig. 12. Temperature profile in the MEA layer at 800 °C average stack temperature steady-state.

Fig. 12 shows the temperatures profiles in the MEA at a steady-state. Radiation effects are not negligible at such high stack temperatures.

The simulation of transient conditions would need the integration of both the electric grid and the control system in the model. This could be a further improvement of the code that could allow also the simulation of failure conditions.

5.4. Cool-down simulation

Considering a simplified stack of few cells results in a pessimistic representation of the actual behaviour of the cool-down (see Section 5). A different approach must be developed to simulate long cool-down time. The time the stack spends to reach the steady-state is deeply influenced by the initial average stack temperature value. The non-operating period can be quite long. The SOFC system has both an high thermal capacity and a very good insulation. Both the stack and the insulation case store a large amount of thermal energy during operating. The rate of such an energy release derives mainly from three quantities: *the heat capacity of the system*, *the insulation thermal conductivity* and *the insulation thickness*. The stack presents a good conductivity in every directions, thus, once the gasses do not flow anymore, the temperature profiles become uniform. While large gradients are expected in the insulation case, the temperature gradients in the stack will be nearly zero in every directions $k_{ins} \ll k_{st}$. From the previous argumentation, the following assumptions can be done: for the cool-down phase the stack can be considered as a homogenous box characterised by averaged value of the heat capacity and the thermal conductivity. Under these approaches a simplified model can be

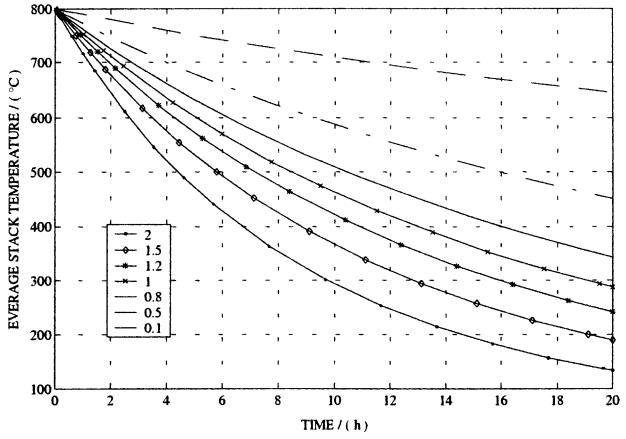

Fig. 13. 20 h coot own simulation s for different value of k_{ins}/s_{ins} (W/(m^2 K)).

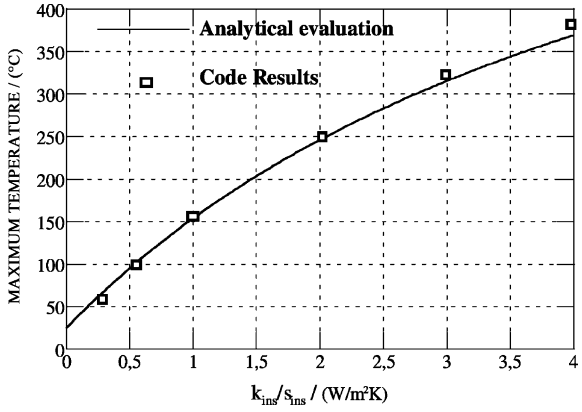

Fig. 14. Maximum outer temperature as a function of k_{ins}/s_{ins} $h_{conv} = 5$ W/(m^2 K); $T_{env} = 25$ °C; $T_{st} = 800$ °C.

performed in order to simulate long cool-down times with contained code run time.

5.4.1. The COOL code

A simplified code has been performed for the cool-down simulation. Cool-down has been simulated with an initial condition corresponding to the temperature profile induced by a steady-state operation at 800 °C. The performances of the insulation system have been tested varying three quantities characterising the cool-down phase (see Section 5.4). The main performances are: (1) *the cool-down time*: long cool-down time induce a reduction in the heat-up and start-up time at every car utilisation; (2) *the outer maximum temperature*: since the SOFC will be installed beside the boot of a car, the outer temperature of the insulation case must be under certain values (about 100 °C).

Once the stack heat capacity is fixed, the k_{ins}/s_{ins} ratio is the main parameter. Actually, the heat capacity of the whole SOFC system is influenced by the s_{ins} value. This effect is not relevant, as the specific heat capacity of the stack is much higher than the insulation one (Table 1).

In Fig. 13 the decreasing of the average stack temperature over 20 h (which is a reasonable time between two consequent utilisations of the car) is shown.

The actual system configuration is characterised by a k_{ins}/s_{ins} ratio of about 1.2 W/(m^2 K), the ratio for a vacuum-multifoil material apparatus (developed for lithium/iron sulphide batteries) is about 0.1 W/(m^2 K) [9]. Increasing the performances of the insulation apparatus also increases the cost very much.

Fig. 14 shows that to achieve an outer temperature of 100 °C at least a k_{ins}/s_{ins} ratio of 0.6 W/(m^2 K) is necessary (assuming only natural convection on the outer surface). While forced cooling would be available when the car is in motion, during cool-down the outer surfaces can be cooled only by natural convection (it would be difficult to utilise a fan cooling system for long periods when the car is switched off). Thus, the k_{ins}/s_{ins} ratio must be under 0.6 W/(m^2 K) to keep the outer temperature under 100 °C.

5.4.2. Analytical evaluation of the insulation case outer temperature

Fig. 15 qualitatively shows the temperature profile into the SOFC during cool-down period. Assuming the conduction with outer air is negligible the following rough equation can be write (in steady-state conditions):

$$k_{ins}\frac{(T_{st} - T_{ins,out})}{s_{ins}}\mathrm{Sup}_{ins} = h_{conv}\mathrm{Sup}_{ins}(T_{ins,out} - T_{env}) \quad (25)$$

The stack temperature can be considered uniform (Section 5.4) and insulation inner temperature is roughly equal to stack temperature (the main heat-transfer mechanism is radiation):

$$k_{ins}\frac{(T_{st} - T_{ins,out})}{s_{ins}}\mathrm{Sup}_{ins} = h_{conv}\mathrm{Sup}_{ins}(T_{ins,out} - T_{env}) \quad (26)$$

By this approximate expression, it is possible to calculate the maximum outer temperature as a function of the parameters characterising the insulation apparatus:

$$T_{max} = \frac{h_{conv}T_{env} + (k_{ins}/s_{ins})T_{st}}{h_{conv} + (k_{ins}/s_{ins})} \quad (27)$$

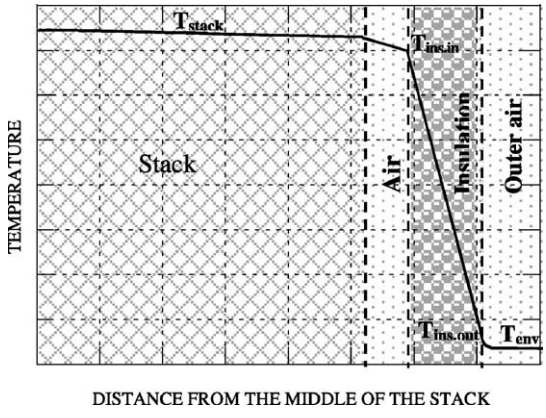

Fig. 15. Qualitative temperature profile during cool-down.

Fig. 14 demonstrates that the results of COOL code are in agreement with such an analytical expression. The h_{conv} dependence on surface temperature is neglected.

6. Conclusion

The results of the simulations demonstrate that mathematical modelling and analysis are a powerful tool to optimise cell design and manufacturing, allowing to investigate the effect and the relative importance of various processing and operating parameters. Especially at the first level of development this model can give precious indications about the device layout, geometry and materials. Simulations can also direct experimentation. Some analytical checks (Section 5.4.2) and comparisons with literature features [10] have been done and they demonstrated the reliability of the results. Some important issues can be deduced from these first simulations:

- A heat exchanger is necessary to reduce the heat-up time, limiting the temperature gradients.
- The air mass flow seems to be the most appropriated regulating parameter to manage heat-up, start-up and steady-state operating.
- Heat-up and start-up times are not adequate for an APU application. It could be necessary to provide the system with the possibility to deliver electric power directly from the engine before steady-state operating of the APU.
- The insulation apparatus requires improvement. Simulations have demonstrated that the average stack temperature falls down too rapidly respect to periods over which cars are usually not utilised.
- The apparatus, which has been simulated, is not adequate to keep the maximum outer insulation temperature under the standard safety value: a reduction of the k_{ins}/s_{ins} ratio allows to achieve this goal avoiding the utilisation of an active cooling system.

Some possible improvements of the code are:

- A stricter evaluation of polarisations (especially for CO electrochemical reaction).
- The extension to coflow and counterflow configurations.
- The introduction of control system and electric external devices in the model.

The modular structure of the code should make such improvements easier.

Acknowledgements

The authors would like to thank Dipl.-Ing. Olav Finkenwirth and Dr. Ing. Franz-Josef Wetzel at BMW AG for their valuable contribution.

References

[1] Fuel Cell Handbook (9.18), US Department of Energy, USA, 2000.
[2] N.Q. Minh, T. Takahaschi, Science and Technology of Ceramic Fuel Cells, Elsevier, Amsterdam, 1995, p. 208.
[3] T. Setoguchi, K. Okamoto, K. Eguchi, H. Arai, J. Electrochem. Soc. 139 (1992) 2875.
[4] E. Achenbach, Three-dimensional and time-dependent simulation of a planar solid oxide fuel cell stack, J. Power Sources 49 (1994) 338–348.
[5] K. Kordesch, G. Simader, Fuel Cells and their Applications, VCH Publishers Inc., New York, 1996 (Chapter 3).
[6] N.F. Bassette II, W.J. Wepfer, J. Winnick, A mathematical model of a solid oxide fuel cell, J. Electrochem. Soc. 142 (1995) 3794.
[7] R.C. Reid, J.M. Prausnitz, B.E. Poling, The Properties of Gasses and Liquids, McGraw-Hill, New York, 1987.
[8] A Malandrino, N. Mancini, Start-up and Load Changes Dynamic Modelling in SOFC System, ENIRICERCHE Press, 1995.
[9] Y. Chen, J.W. Evans, Cool-down time of SOFCs intended for transportation application, J. Power Sources 58 (1996) 90.
[10] J. Palsson, A. Selimovic, L. Sjunnesson, J. Power Sources 86 (2000) 442.